New Heterometallic Compound as Luminescent Sensor for Detection of CS_2 and Treatment Effect on Childhood Diabetes

Wen-Hui Sun
Shandong University
Bing Ye (Yebing2021@126.com)
Shandong University https://orcid.org/0000-0003-3731-2991

Research Article

Keywords: Heterometallic compound, Luminescence sensing, childhood diabetes

Posted Date: June 7th, 2021

DOI: https://doi.org/10.21203/rs.3.rs-556025/v1

Version of Record: A version of this preprint was published at Journal of Fluorescence on April 20th, 2022. See the published version at https://doi.org/10.1007/s10895-022-02943-0.

Abstract

The hydrothermal reaction of $Cd(NO_3)_2{\cdot}4H_2O$, KNO_3 with the dicarboxylate ligand of 2-aminoterephthalic acid (H_2L) yields a new heterometallic coordination polymer with the formula of $[CdK_2(L)_2(H_2O)_4]_n$ (**1**). Compound **1** emits intense luminescence at ambient temperature and shows high selectivity and sensitivity for the detection of CS_2. Serial biological experiments were conducted to evaluate the activity of the new compound on children diabetes. First of all, after the compound treatment, the blood glucose meter was used to measure the levels of body's blood sugar. In addition to this, the relative expression levels of the insulin receptor on the liver cells were determined with real time RT-PCR.

Introduction

With the development of society and economy, the improvement of people's living standards and the change of lifestyle, the incidence of diabetes in children has an increasing trend in recent years just like adults [1]. The global incidence of childhood diabetes varies greatly, the Europe and the United States having a lower incidence than Southeast Asia, and Asia having the lowest incidence [2]. The age of childhood diabetes onset is generally 10–14 years old, which needs to arouse the attention of clinicians.

As a colorless volatile chemical solvent, carbon disulfide (CS_2) has been extensively used in industry for the production of carbon tetrachloride, vulcanized rubber, glass paper, viscose fiber, and pesticide [3]. When humans are exposed to high levels of CS_2, it could lead to atherosclerosis and coronary artery disease owing to its high toxicity [4]. As a result, it is urgent to seek more convenient and selective methods for the detection of CS_2. During the past few decades, metal-organic frameworks (MOFs) have rapidly developed as new kind of functional crystalline materials [5–8]. Numerous of MOFs with intense luminescence have been successfully prepared, which show excellent sensing properties for the detection of volatile organic solvent, nitroaromatic explosives and toxic heavy metal ions [9–12]. Compared with transitional detection methods, luminescence-based method with MOFs has some advantages of high sensitivity, easy operation, and visualization [13]. However, it is still a great challenge to construct thermostable MOFs with intense luminescence emission for the detection of harmful substances. Polycarboxylate ligand have been widely used for the construction of MOFs because of their versatile coordination modes toward metal ions [14–16]. The metal ions can be easily connected by the carboxylate groups into rod-shaped substructure [17, 18]. The ordered stack of the rod-shaped substructures helps to increase the stabilities of MOFs. Considering that, in this work, 2-aminoterephthalic acid was selected as the organic block to assemble with Cd(II) and K(II) ions, successfully prepared a new heterometallic compound, namely $[CdK_2(L)_2(H_2O)_4]_n$ (**1**). What is interesting is that compound **1** shows high selectivity and sensitivity for the detection of CS_2 *via* luminescence quenching. After serial different biological experiments, the application values of compound on the children diabetes were explored, and the related mechanism discussed at the same time.

Experimental

Materials and instrumentation

All reagents and solvents used in this work were of analytical grade and used without further purification. Elemental analyses (C, H and N) were determined using an elemental Vario EL III analyzer. Powder X-ray diffraction (PXRD) analysis were recorded on a PANalytical X'Pert Pro powder diffractometer with Cu/Kα radiation (λ = 1.54056 Å) with a step size of 0.05°. Thermogravimetric analysis for compounds **1** were performed on a NETSCHZ STA-449C thermoanalyzer with a heating rate of 10 ℃/min under air atmosphere in the temperature range of 30–800℃. The luminescent properties of **1**, H_2L and phen were investigated using the Edinburgh Analytical instrument FLS920.

Synthesis of compound $[CdK_2(L)_2(H_2O)_4]_n$ ((1)

A mixture of $Cd(NO_3)_2{\cdot}4H_2O$ (0.100 mmol), KNO_3 (0.1 mmol) H_2L (0.100 mmol), $NaHCO_3$ (0.20 mmol) and H_2O (10.0 mL) was sealed into a 25.0 mL Teflon-lined high-pressure container and held at 150 ℃ for 72 h. After cooling to the room temperature at a rate of 2 ℃/min, yellow block crystals of **1** were obtained in 38% yielding based on H_2L. Elemental analysis Calcd. for $C_{16}H_{12}CdK_2N_2O_{10}$ (Mr = 582.89): C, 32.94; H, 2.06; N, 4.80%. Found: C, 32.97; H, 2.03; N, 4.83%.

X-ray crystallography

Single crystal data of **1** was collected on a computer–controlled Oxford Xcalibu E diffractometer with graphite–monochromated Mo–*Kα* radiation (λ = 0.71073 Å) at T = 293(2) K. The structure of **1** was solved by the dual direct method and further refined with the full-matrix least square technique based on F^2 using the *SHELXL*-2014 [19]. Crystallographic data of compound **1** are summarized in Table 1. Selected bond lengths (Å) and angles (º) of **1** are listed in Table S1.

Table 1
The Crystal data for compound **1**.

Formula	$C_{16}H_{12}CdK_2N_2O_{10}$
Fw	582.89
Crystal system	tetragonal
Space group	$I4_1/acd$
a (Å)	21.298(2)
b (Å)	21.298(2)
c (Å)	12.211(2)
α(°)	90
β(°)	90
γ(°)	90
Volume (Å^3)	5538.8(16)
Z	8
Density (calculated)	1.398
Abs. coeff. (mm^{-1})	1.132
Total reflections	9168
Unique reflections	1576
Goodness of fit on F^2	1.111
Final *R* indices [$I > 2\text{sigma}(I^2)$]	$R = 0.0807$, $wR_2 = 0.2286$
R (all data)	$R = 0.1031$, $wR_2 = 0.2518$
CCDC	2082357

Sensing experiments

The powder samples of **1** (4 mg) were separately immersed into 4 mL different solvent of H_2O, DMF (N,N-dimethylformamide), DMA (N,N-dimethylacetamide), MeOH, EtOH, THF (tetrahydrofuran), CH_3CN, acetone, EG (ethylene glycol), and CS_2, and then the above suspensions were ultrasonically treated for five minutes. After that the suspension was placed in a quartz cell of 1 cm width for fluorescence detection. The titration experiments were performed by gradual addition of CS_2 into DMF solution.

Blood glucose measurement

The blood glucose meter was used to measure the levels of body's blood sugar after model construction and compound treatment. This preformation was finished totally under the guidance of the instructions with some modifications. In brief, 50 Balb/c mice (3 weeks, 13–16 g) used in this research were obtained from the Model Animal Research Center of Nanjing University (Nanjing, China), and then kept at standard condition of 45% humidity and 20–25℃ temperature. The mice were fed with high fat feed to induce the diabetes animal model. When the bold glucose ≥ 16.7mmol/L, it was regarded as the successful model construction. Next, the compound was injected for treatment at the concentration of 1, 2 and 5 mg/kg. The blood of all the mice were harvested and the blood glucose was measured at the 3rd and 7th day after compound treatment.

Real time RT-PCR

The relative expression levels of the insulin receptor on the liver cells after compound treatment was measured with real time RT-PCR. This conduction was finished strictly in accordance with the protocols with only a little change. In short, 50 Balb/c mice (3 weeks, 13–16 g) used in this research were obtained from the Model Animal Research Center of Nanjing University (Nanjing, China), and then kept at standard condition of 45% humidity and 20–25℃ temperature. The mice were fed with high fat feed to induce the diabetes animal model. When the bold glucose ≥ 16.7mmol/L, it was regarded as the successful model construction. Next, the compound was injected for treatment at the concentration of 1, 2 and 5 mg/kg. After the treatment, the liver tissue of the mice was harvested and the total RNA in the cells was extracted with TRIZOL reagent. The concentration of the total RNA was measured, followed by the reverse transcription into cDNA. Finally, the relative expression of the α receptor on liver cells was measured with RT-PCR, the *gapdh* was as the internal control gene.

Results And Discussion

Crystal structure of compound 1

X-ray crystallography analysis indicates that compound **1** features a 3D heterometallic framework that crystallizing in tetragonal $I4_1/acd$ space group. Each asymmetric unit of **1** is composed of one forth Cd(II) ion, half K(I) ion, half L^{2-} ligand, as well as one coordinated water molecule. The Cd1 ion bonds to eight oxygen atoms from four carboxylate groups of four independent L^{2-} ligands, affording a distorted tetragonal antiprism, and the K1 ion bonds to one terminal water ligand and three carboxylate oxygen atoms from three different L^{2-} ligands, generating a distorted tetrahedron (Fig. 1). The Cd-O bond distances range from 2.336(4) to 2.517(5) Å, and the K-O bond lengths are in the range of 2.692(5)-2.708(5) Å. Each L^{2-} ligand adopts a $(\mu_2\text{-}\mu_2)\text{-}(\mu_2\text{-}\mu_2)\text{-}\mu_6$ coordination mode linking with two Cd(II) ions and four K(I) ions (Fig. S1). In the structure of **1**, each $\{CdO_8\}$ polyhedron shares four edges with four adjacent $\{KO_4\}$ tetrahedrons, and each $\{KO_4\}$ tetrahedron shares two edges with two adjacent $\{CdO_8\}$ polyhedrons, these connectivities further link the polyhedrons into a 1D chain extending along crystallographical *b* direction (Fig. 2a). Finally, these 1D infinite 1D chains are connected by the L^{2-}

ligands, giving rise to a 3D heterometallic framework (Fig. 2b). Calculated by PLATON, it can be found that the framework of 1 contains 25.5% solvent accessible volume (1391.8 $Å^3$ total accessible volume/5538.8 $Å^3$ per unit cell volume).

Powder X-ray diffraction pattern (PXRD) and thermogravimetric analysis (TGA)

The experimental and simulated PXRD patterns are shown in Fig. S2a. It is obvious that the experimental pattern matches well with the simulated one generated from the single crystal diffraction data, indicating that the crystal structure of **1** is truly representative of the obtained bulk samples.

The TGA curve of **1** was shown in Fig. S2b. It displays two-step weight loss process. The first weight loss is 12.31% occurring in the range of 72–117°C that can be assigned to the removal of the coordinated water molecules (calcd: 12.35%), and the second occurred ranging from 300 to 410°C with a weight loss of 49.48% that can be attributed to the decomposition of the organic ligand (calcd: 49.5%).

Photoluminescent sensing properties of 1

The solid-state luminescent spectra of **1** and free H_2L were measured at room temperature (Fig. S3). Compound **1** shows intense luminescence with emission band centered at 456 nm (λ_{ex} = 350 nm), and the free H_2L has an emission band at 436 nm (λ_{ex} = 340 nm) that was caused by intraligand $\pi^* \rightarrow \pi/n$ electron migration transitions. Based on the reported literature [20], the luminescence origin of **1** can be tentatively assigned to intraligand charge transfer. Compared to that of the free H_2L ligand, the obvious red-shift of 20 nm for **1** may be closely related to the coordination of L^{2-} ligand to central metal ions.

The intense emission and good thermal stability of **1** further impelled us to investigate its sensing properties for different solvent molecules. The luminescence intensities of **1** dispersed in different organic solvent were measured at room temperature. As shown in Fig. 3a, the solvents of H_2O, DMF, DMA, MeOH, and EtOH showed negligible effect on the luminescence intensity of **1**. In the case of THF, CH_3CN, acetone and EG, the luminescence intensity of **1** decreased with quenching efficiencies ranging from 27.5–51.6%. Interestingly, we found that the luminescent intensity of **1** was almost completely extinguished when dispersed in CS_2. These results imply that compound **1** has highly selective detection ability toward CS_2. Then, the sensing sensitivity of **1** toward CS_2 was further investigated *via* the titration experiment by addition of 10 ppm CS_2 each time. As shown in Fig. 4b, the luminescence intensities of **1** decreased gradually upon the addition of CS_2, and when the CS_2 concentration is up to 110 ppm, the luminescence of **1** was almost completely quenched with a high quenching efficiency of 95.92%. Moreover, the detection limit of **1** toward CS_2 was calculated with $3\sigma/k$ (k: slope, σ: standard) *via* a linear fitting in the concentration range of 0–60 ppm, and the value of detection limit for CS_2 is calculated to be about 0.113 ppm (Fig. S4), indicating that compound **1** exhibits high detection sensitivity toward CS_2. After luminescence sensing of CS_2, the structural skeleton of **1** remains intact that was demonstrated by

the PXRD experiment (Fig. S2a). Thus, compound **1** can be served as a structurally stable sensing material for the detection of CS_2 with high selectivity and sensitivity.

Compound significantly reduced the body blood glucose levels of dose and time dependently

For the treatment of the children diabetes, the compound with new structure was synthesized in this research, and its inhibitory activity on the increased blood glucose levels was determined with blood glucose meter. As the results showed in Fig. 4, we can see that the there was a significantly increased level of blood glucose in the model group than the control group, with $P < 0.005$. After the treatment of the new compound with 1, 2 and 5 mg/kg, the levels of body blood glucose in the diabetes mice was reduced in a dose and time dependent manner. This result showed that the compound has excellent application values on the diabetes treatment.

Compound obviously inhibited the relative expression of the insulin receptor on liver cells

As introduced above, the new compound could obviously reduce the body blood glucose in a dose and time dependent manner. As the insulin receptor on the liver cells could significantly regulate the body's blood sugar. Thus, the real time RT-PCR was conducted and the content of the insulin receptor on the liver cells was measured. The results in Fig. 5 showed that the relative expression of the insulin receptor on the liver cells of the model group was much lower than that of the control group. After the treatment of the new compound, the content of the insulin receptor on the liver cells was significantly increased. This promotion of the new compound exhibited a dose and time dependent relationship.

Conclusion

In summary, a new heterometallic compound of $[CdK_2(L)_2(H_2O)_4]_n$ (**1**) has been hydrothermally prepared and structurally characterized by the single crystal structural analysis. It features a 3D framework with 25.5% solvent accessible volume. Investigations of luminescence sensing property for **1** show that it can highly selective and sensitive sensing of CS_2 under room temperature. The results of the blood glucose determination showed that the compound could significantly reduce the levels of body blood glucose dose and time dependently. In addition to this, the results of the real time RT-PCR indicated that the relative expression of the insulin receptor on the liver cells was also inhibited by the new compound. Above all, we draw this conclusion, the compound has the potential to be an excellent candidate for the children diabetes by up-regulating the insulin receptor levels on the liver cells.

Declarations

Funding

Not applicable.

Conflicts of interest

All authors declare that there is no conflict of interest regarding the publication of this paper.

Ethics approval

We try to replace live animals with unconscious experimental materials, or use lower animals to replace higher animals. we try to use the smallest number of animals to get the same amount of experimental data or use a certain number of animals to get more experimental data. We minimize the scope and extent of the impact of inhumane procedures on animals. All the preformation conducted in this present research was approved by the Animal Ethics Committee of Affiliated Hospital of Nanjing University (Nanjing, China) with the No. 20200233.

Consent to participate

Not applicable

Consent for publication

Written informed consent for publication was obtained from all participants

Availability of data and material

Selected bond lengths (Å) and angles (°) for **1** (Table S1); The coordination mode of L^{2-} ligand in **1** (Fig. S1); PXRD patterns of **1** (a), TGA curve of **1 (b)** (Fig. S2); The luminescent emission spectra of **1** and free H_2L ligand at room temperature (Fig. S3); The detection limit of **1** toward CS_2 (Fig. S4), the information could be found in the supporting information file.

Code availability

The data that support the findings of this study have been deposited in NCBI Reference Sequence: NC_000002.12.

Authors' contributions

Wen-Hui Sun carried out the experiments, analyzed the data and wrote the draft of this manuscript; Bing Ye designed the whole experiments and revised the draft.

References

1. Ziegler R, Neu A. Diabetes in Childhood and Adolescence. Dtsch Arztebl Int. 2018; 115: 146-156.

2. Haliloğlu B, Abalı S, Buğrul F, Çelik E, Baş S, Atay Z, Güran T, Turan S, Bereket A. The Distribution of Different Types of Diabetes in Childhood: A Single Center Experience. J Clin Res Pediatr Endocrinol. 2018; 10: 125-130.
3. Yan, C. Wang, Z. Zheng, L. Qu, D. Zeng, M. Li, Renal injury following long-term exposure to carbon disulfide: analysis of a case series. *BMC Nephrol*., **2019**, *20*, 377.
4. Phillips, Detection of carbon disulfide in breath and air: a possible new risk factor for coronary artery disease. *Int. Arch. Occup. Environ. Health*, **1992**, *64*, 119.
5. Gao, J. Zhang, L. Zhai, J. Liang, J. Liang, X. Niu, T. Hu, Fluorescent sensing properties of Cd(II)/Zn(II) metal-organic frameworks based on 3,5-di(2',5'-dicarboxylphenyl)benozoic acid. *Polyhedron*, **2019**, *164*, 90.
6. Q. An, C. C. Zhang, L. J. Duan, X. Y. Liu, Z. Wang, X. Y. Jin, W. M. Song, Luminescent metal-organic framework with a 2-(4-pyridyl)-terephthalic acid ligand for detection of acetone. *New. J. Chem*., **2019**, *43*, 4800.
7. H. Chang, Y. Zhao, M. L. Han, L. F. Ma, L. Y. Wang, Five Cd(II) coordination polymers based on 2,3',5,5'-biphenyltetracarboxylic acid and N-donor coligands: syntheses, structures and fluorescent properties. *CrystEngComm*, **2014**, *16*, 6417.
8. R. Li, J. Sculley, H. C. Zhou, Metal-organic frameworks for separations. *Chem. Rev*., **2012**, *112*, 869.
9. Wu, Y. Liu, Y. Liu, J. Wang, Y. Li, W. Liu, J. Wang, Cadmium-based metal-organic frameworks as a highly selective and sensitive ratiometric luminescent sensor for mercury(II). Inorg. Chem., **2015**, *54*, 11046.
10. F. Li, M. L. Zhu, L. P. Lu, A. Wang, A novel monocapped square-antiprismatic Ba(II) coordination polymer: a design for dual-responsive fluorescent chemosensor for $Cr_2O_7^{2-}$ and Fe(III). J. Solid State Chem., 2020, 290, 121582.
11. K. Singha, P. Majee, S. Hui, S. K. Mondal, P. Mahata, Luminescent metal-organic framework-based phosphor for the detection of toxic oxoanions in an aqueous medium. *Dalton Trans*., **2020**, *49*, 829.
12. J. Wang, F. F. Wu, N. Su, P. P. Li, S. Y. Wang, H. Y. Ma, Y. W. Li, M. H. Yu, Luminescent coordination polymers constructed using a mixed-ligand strategy for highly selective luminescence sensing of nitrobenzene, Fe^{3+} and $Cr_2O_7^{2-}$ ions and photodegradation of rhodamine B. *CrystEngComm*, **2020**, *22*, 4650.
13. F. Wu, B. Tan, M. L. Feng, A. J. Lan, X. Y. Huang, A magnesium MOF as a sensitive fluorescence sensor for CS_2 and nitroaromatic compounds. *J. Mater. Chem. A*, **2014**, *2*, 6426.
14. Zhang, Z. J. Li, Q. P. Lin, Y. Y. Qin, J. Zhang, P. X. Yin, J. K. Cheng, Y. G. Yao, Synthesis, structure, and luminescent properties of hybrid inorganic-organic framework materials formed by lead aromatic carboxylates: inogranic connectivity variation from 0D to 3D. *Inorg. Chem*., **2009**, *48*, 6517.
15. Du, M. Zhao, X. Long, S. Du, A new acentric heterometallic inorganic-organic hybrid framework with an unusual {Cd3Na4} array: NLO and ferroelectric properties. *Inorg. Chem. Commun*., **2013**, *38*, 39.

16. Lu, J. Wang, C. Y. Shi, X. D. Jiang, Y. C. Sun, W. P. Wu, W. X. Hu, Four new coordination complexes prepared for the degradation of methyl violent dye based on flexible dicarboxylate and different N-donor coligands. *J. Mol. Struct.*, **2021**, *1225*, 129181.
17. Zhang, Y. Y. Huang, Q. P. Lin, J. Zhang, Y. G. Yao, Using alkaline-earth metal ions to tune structural variations of 1,3,5-benzenetricarboxylate coordination polymers. Dalton Trans., 2013, 42, 2294.
18. P. He, Y. X. Tan, J. Zhang, Gas sorption, second-order nonlinear optics, and luminescence properties of a series of lanthanide-organic frameworks based on nanosized tris((4-carboxyl)phenylduryl)amine ligand. Inorg. Chem., 2013, 52, 12758.
19. M. Sheldrick, *Acta Crystallogr., Sect. C: Struct. Chem.*, **2015**, *71*, 3.
20. Zhang, Y. Y. Huang, J. K. Cheng, Y. G. Yao, J. Zhang, F. Wang, Alkaline earth metal ion doped Zn(II)-terephthalates. *CrystEngComm*, **2012**, *14*, 4843.

Figures

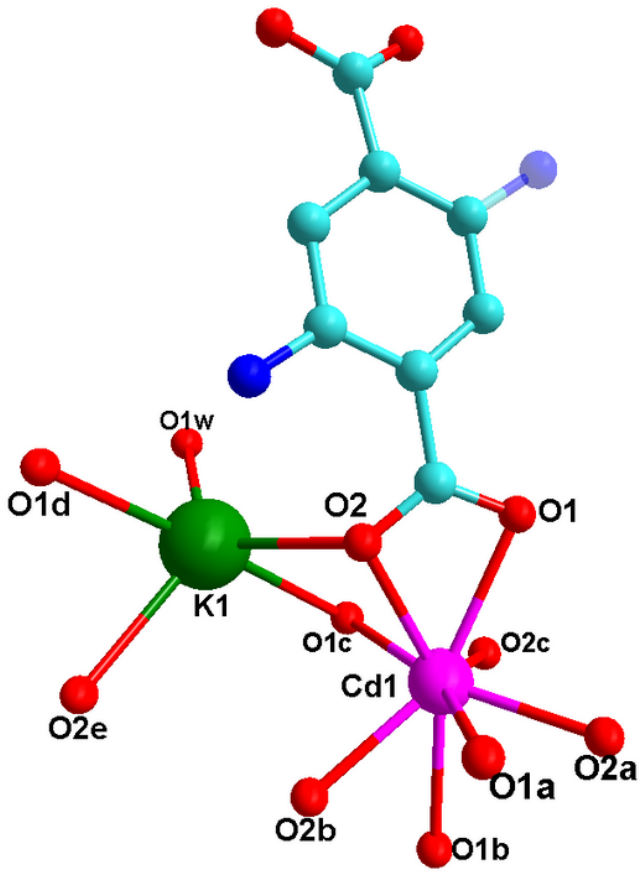

Figure 1

Viewing of the coordination environments of Cd(II) and K(I) ions in 1 (symmetry codes: (a) 0.25 + x, 0.75 − y, 0.25 − z; (b) 1 − x, 0.5 − y, z; (c) 0.75 − y, −0.25 + x, 0.25 − z; (d) 1 − x, y, 0.5 + z; (e) 0.75 − y, 0.75 − x, 0.75 − z).

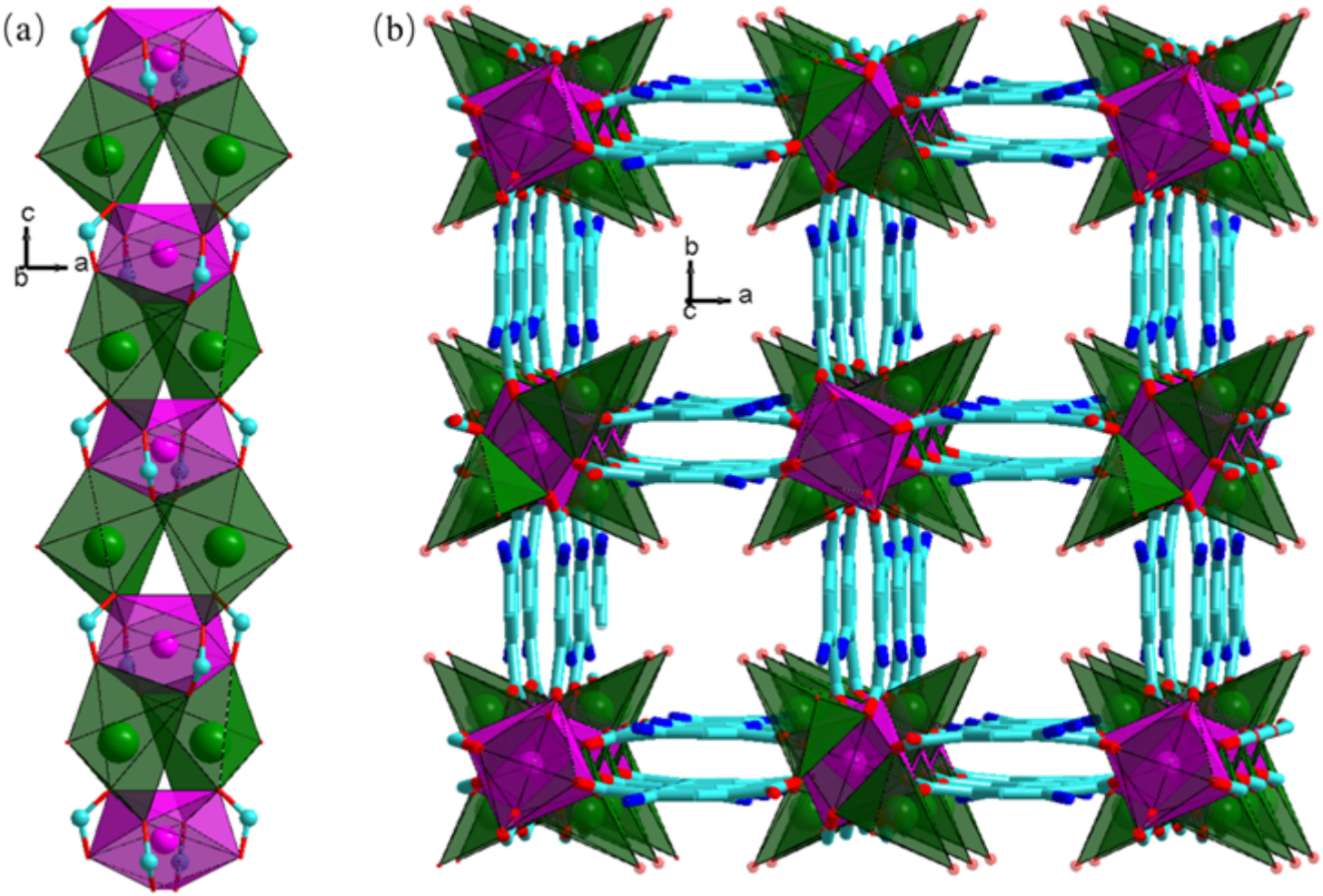

Figure 2

(a) 1D chain motif constructed by the {CdO8} and {KO4} polyhedrons. (b) A polyhedral representation of the 3D framework of 1.

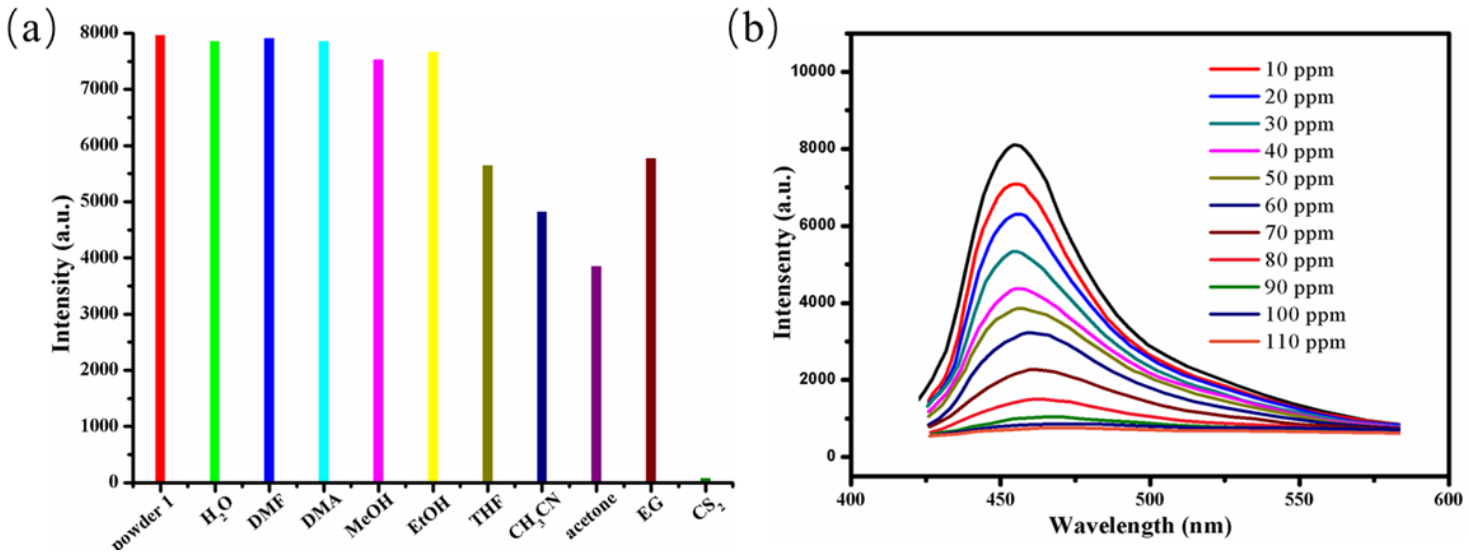

Figure 3

(a) Luminescent emission intensities of 1 dispersed in different solvents. (b) Emission spectra of 1 dispersed in DMF with different concentration of CS2.

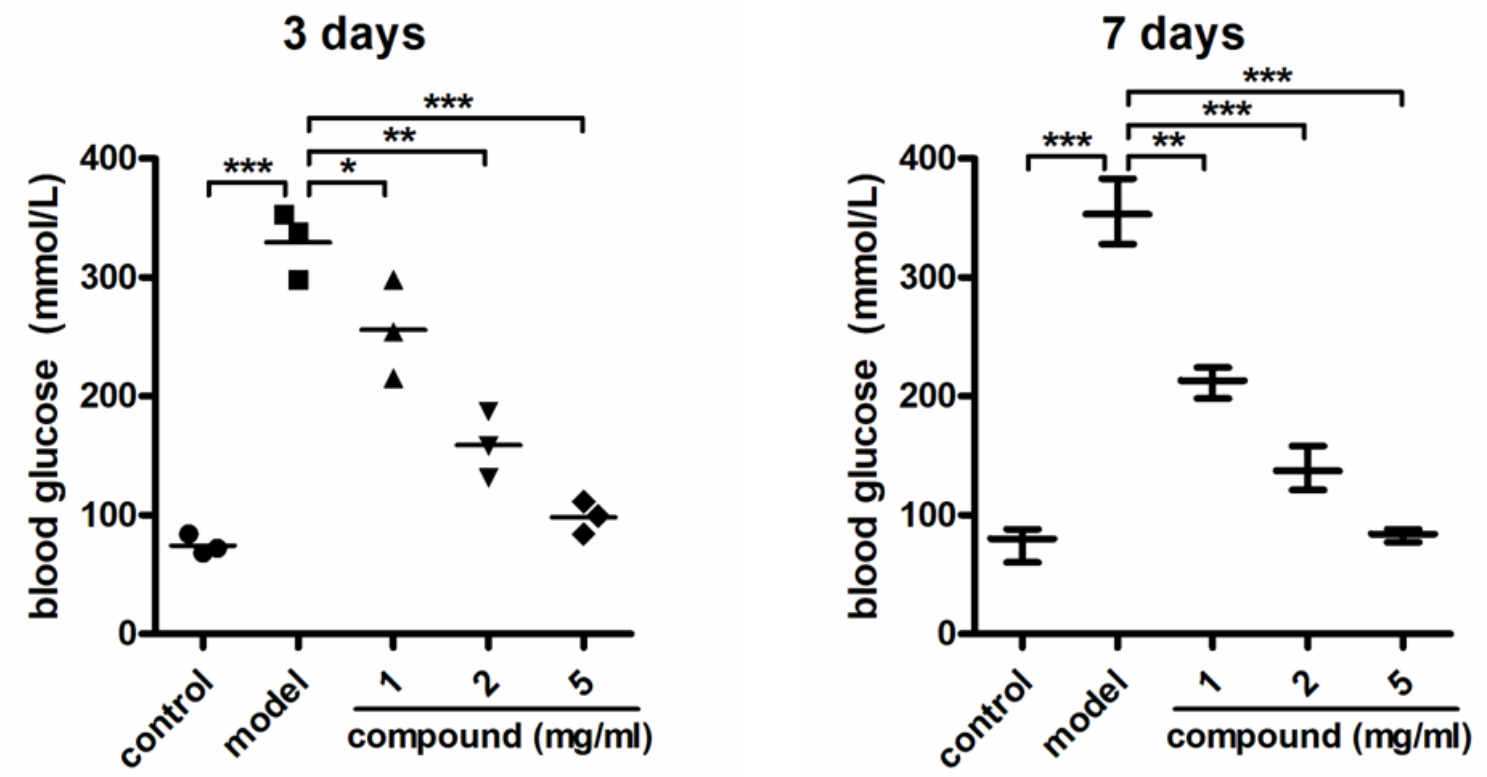

Figure 4

Significantly reduced body blood glucose levels of dose and time dependently by the new compound. The diabetes mice model was constructed and then the compound was given for treatment at the concentration of 1,2 and 5 mg/kg. The blood glucose meter was used to measure the levels of body's blood sugar.

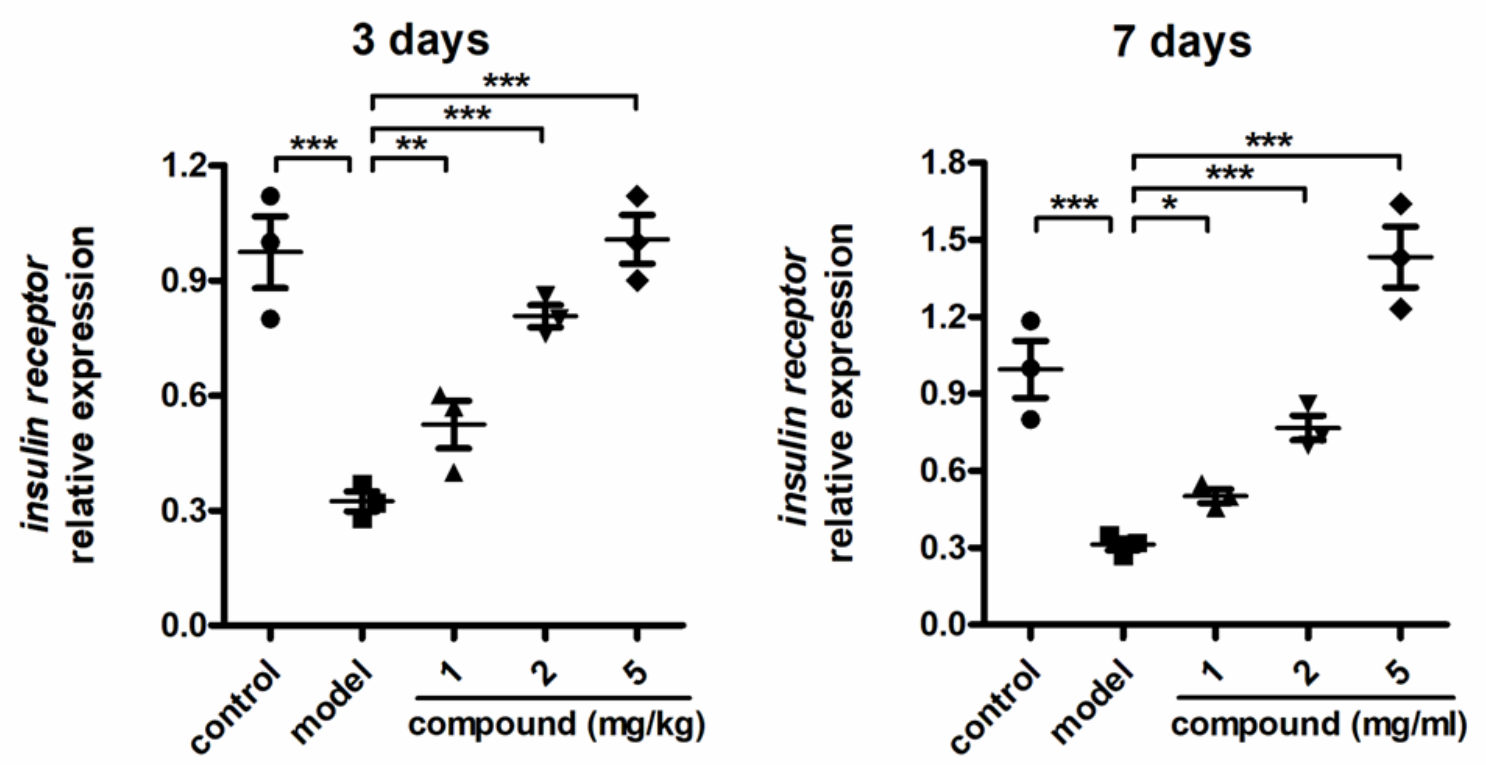

Figure 5

Obviously inhibited relative expression of the insulin receptor on liver cells after compound treatment. The diabetes mice model was constructed and then the compound was given for treatment at the concentration of 1, 2 and 5 mg/kg. The real time RT-PCR was conducted and the relative expression of the insulin receptor was determined.

Supplementary Files

This is a list of supplementary files associated with this preprint. Click to download.

- SupplementaryMaterial.doc